IL-18 activates mucosal group 2 innate lymphoid cells following enteric bacterial infection

Rita Berkachy[1], Vishwas Mishra[1], Priyanka Biswas[1], Zuza Kozik[2], Jyoti Choudhary[2]

Gad Frankel[1*]

[1]Department of Life Sciences, Imperial College London, London SW7 2AZ, UK

[2]Functional Proteomics Group, Chester Beatty Laboratories, Institute of Cancer Research, London, United Kingdom

For correspondence: g.frankel@imperial.ac.uk

Abstract

Group 2 innate lymphoid cells (ILC2s) are traditionally associated with immune responses to helminth infection and mediating allergic inflammation via the production of type 2 cytokines. However, little is currently known about activation of ILC2s in response to bacterial infection. Here we show that colonic lamina propria ILC2s proliferate in response to infection with the enteric mouse pathogen *Citrobacter rodentium*, which is used to model infections with enteropathogenic and enterohaemorrhagic *Escherichia coli*. We also show that following infection, the colonic lamina propria ILC2s secret IL-4, IL-5 and IL-13. We demonstrate that, in addition to IL-33, colonic ILC2s are activated by IL-18, with both cytokines being upregulated in *C. rodentium*-infected gut. Whilst *C. rodentium* did not induce ILC2 proliferation in IL-22 KO mice, this was reversed by administration of IL-18. Conversely, injection of IL-18 binding protein into *C. rodentium*-infected wild type mice blocked activation of ILC2s. These data show that ILC2s are activated in response to bacterial gut infection, where proliferation and activation of ILC2s can be mediated via IL-18 induced by IL-22 signalling.

Introduction

In the last fifteen years, a growing family of the innate immune system has been described, termed innate lymphoid cells (ILCs). ILCs are antigen-receptor negative cells, activated by cytokine signals and enriched in mucosal surfaces, where they form a first line of defence against pathogenic threats defence against pathogenic threats (1-3). These innate counterparts of helper T cells shape early immune responses through production of various cytokines. In addition to their immediate response to infections and their interaction with adaptive immune cells, ILCs facilitate the maintenance of barrier integrity and can contribute to wound healing and tissue repair in the lungs and gut following injury (4). Based on their development and function, ILCs are classified into five subsets: natural killer (NK) cells, group 1 ILCs (ILC1s), group 2 ILCs (ILC2s), group 3 ILCs (ILC3s) and lymphoid tissue inducer cells (LTis) (4). Furthermore, the ILC lineages are inherently plastic and can transdifferentiate to other ILC subtypes in response to local cytokine and/or environmental cues (5, 6).

NK are cytotoxic cells that circulate in the bloodstream, killing virus-infected cells and providing tumour surveillance. When activated, they secrete granzymes and perforin, inducing apoptosis in targeted cells (7). ILC1s are non-cytotoxic tissue-resident cells (8-10) that respond to various viruses and can also play a role in certain bacterial and parasitic infections such as *Clostridium difficile* (11) and *Toxoplasma gondii* (12). Upon activation, both NK cells and ILC1s express the transcription factor T-bet (encoded by *Tbx21*) and secrete interferon gamma (IFNγ). ILC2s are vital for the immunity against extracellular helminth parasites. Alarmins such as IL-25, IL-33 and thymic stromal lymphopoietin (TSLP) induce production of the type 2 cytokines IL-4, IL-5, IL-9 and IL-13 by ILC2 (13, 14). During infection with the mouse intestinal parasitic nematode *Nippostrogylus brasiliensis* (*N. brasiliensis*), IL-25 secreted from tuft cells and IL-33 from

damaged intestinal epithelial cells contribute to ILC2 expansion and the secretion of IL-5 and IL-13 (15-17). A recent study showed that stomach ILC2 are activated during *Helicobacter pylori* infection (18). In addition, IL-18 was recently shown to activate resident ILC2s in the skin via the IL-18R1 (CD218) receptor. Whilst this receptor is highly expressed on dermal ILC2s, it was also detected on lung and bone marrow ILC2 populations; importantly, CD218 was not detected in ILC2s in the small intestine (19). ILC3s are involved in mucosal immunity to extracellular bacteria and fungi and are characterised by the production of interleukin (IL)-17, IL-22, and granulocyte macrophage colony-stimulating factor (GM-CSF) (20).

Citrobacter rodentium is a Gram-negative, extracellular, enteric mouse pathogen, used to model infections with the human pathogen enteropathogenic and enterohaemorrhagic *Escherichia coli* (21, 22). Following infection, *C. rodentium* binds intimately to intestinal epithelial cells (IECs), leading to disruption of tight junctions and release of IL-23 and IL-1β from dendritic cells (DCs) and macrophages respectively (23). In turn, IL-23 activates ILC3s resulting in the production of IL-22 and phosphorylation of STAT3, which induces secretion of antimicrobial peptides (AMPs) and mucus, promoting epithelial barrier resistance (24, 25). Infection with *C. rodentium* triggers colonic crypt hyperplasia (CCH), and reprogramming of the metabolic profile in IECs (e.g. bioenergetics and cholesterol haemostasis) and physiology of the mucosal surface (e.g. mucosal barrier function). These changes, which are first detected 4 days post infection (dpi), are amplified at 6 dpi and start to be resolved from 12 dpi, as soon as the pathogen started to be cleared by adaptive immune responses (26, 27).

In this study, we aimed to investigate if resident colonic lamina propria ILC2s respond to infection with extracellular bacterial pathogens, using *C. rodentium* as a model. We show that upon infection, colonic ILC2s proliferate and secrete type 2 cytokines in response to IL-18 stimulation.

Materials and methods

Mice and ethics statement

Female C57Bl/6J mice of 6-10 weeks age were purchased from Charles River UK and IL-22 KO mice were bred in house. All mice were maintained at the Central Biomedical Services (CBS) facility at Imperial in pathogen-free conditions at 20-22 °C and 30-40 % humidity on 12 hours light/dark cycle. All animal procedures were conducted in accordance with Animals Scientific Procedures Act 1986 and U.K. Home Office guidelines and reviewed by the Imperial College Animal Welfare Ethical Review Body (AWERB).

Citrobacter rodentium infection

C. rodentium cultures were prepared in 15 ml LB supplemented with 50 µg/µL nalidixic acid and grown at 37 °C with shaking at 200 rpm. The next day, cultures were centrifuged, resuspended with 1.5 ml phosphate-buffered saline (PBS) and each mouse received 200 µl by oral gavage(28). Uninfected mice (mock infected) received 200 µl of PBS. To quantify the colony forming unit (CFU) per gram of stool, stool samples were plated onto agar plates and viable bacteria were counted as previously described(28). Infected mice that did not reach the threshold of 1×10^7 CFU/g of stool were excluded from further experimental processing and analysis.

In vivo administration of IL-18 and IL-18 binding protein

Recombinant mouse IL-18 (rmIL-18, Cat No. 9139, R&D Systems) and recombinant human IL-18 binding protein (rhIL-18BP, Cat No. 119-BP, R&D Systems) were freshly prepared in PBS and given to mice by intraperitoneal injection, in a volume of 0.1 ml on days 2 and 3 p.i. at a dose of 5 mg/kg and 1 mg/kg respectively. Control groups received PBS only.

Cytokines and antibodies

Recombinant murine cytokines were purchased from PeproTech (IL-2, IL-7, IL-22, IL-25/Il-17E and IL-33) or R&D Systems (IL-18 and TSLP). All cytokines were lyophilised in PBS and stored at -80 °C.

The following antibodies were purchased from Biolegend or BD Biosciences and used for flow cytometry: Fc Block (anti-mouse CD16/CD32 mAb, clone 2.4G2, BD Biosciences), CD3 (145-2C11), B220 (RA3-6B2), CD19 (6D5), TER119 (TER-119), Gr-1 (RB6-8C5), CD5 (53-7.3), FcεRI (Marl), CD11c (N418), F4/80 (BM8), CD45 (30F11), CD90.2 (30-H12), Nkp46 (29A1.4), CCR6 (29-247), CD4 (RM4-5), CD127 (A7R34), KLRG1 (2F1), NK1.1 (PK136), EOMES (W17001A), GATA3 (L50-823), Tbet (4B10), RORγt (Q31-378), IL-4 (11B11), IL-5 (TRFR5), IL-13 (ebio13A), IFNγ (XMG1.2) and Ki67 (SolA15).

Isolation of lamina propria immune cells and IECs from mouse colons

Lamina propria cells were isolated from mouse colons as previously described(29). Briefly, cleaned colons were cut open longitudinally then incubated for 20 min at 37 °C in a shaking incubator in Hanks' balanced salt solution (HBSS; Ca^{2+} and Mg^{2+} free) supplemented with 2% FBS, 10 mM EDTA and 1 mM DTT. Supernatants containing IECs were collected, and cells were stored at −80 °C until processing for RNA extraction. Residual tissues were digested at 37°C for ~40-50 min in RPMI 1640 containing 62.5 μg/mL Liberase, 50 μg/mL DNase I and 2 % FBS. Mononuclear cells were isolated with 40-80% Percoll gradient and washed twice.

Flow cytometry and cell sorting

For the analysis of cytokine expression, isolated cells were stimulated with 1x cell stimulation cocktail (Cat No. 00-4970, eBioscience) for 4 hours at 37 °C/5% CO2 in the presence or absence of 1x protein transport inhibitor cocktail (Cat No. 00-4980, eBioscience).

To stain for extracellular markers, single-cell suspensions or stimulated cells were plated in a 96 well V bottomed plate and stained for 10 min with LIVE/DEAD fixable blue (Thermo Fisher, diluted in D-PBS) to detect and exclude dead cells from subsequent analysis. Cells were then treated for 20 min with Fcγ receptor block followed by surface marker staining using fluorophore-conjugated monoclonal antibodies (BioLegend, BD Biosciences or eBioscience). All incubations were performed at 4°C in the dark, unless otherwise stated. Negative (unstained and live/dead) along with fluorescent-minus-one (FMO) controls were considered to estimate background fluorescence.

For intracellular staining, cells were first fixed for 20-30 min at room temperature in the dark, using the eBioscience Forkhead box protein 3 (Foxp3)/transcription factor fixation buffer set to stain for transcription factors or the IC fixation buffer for the detection of intracellular cytokines. Fixed cells were then stained for 1 hr with intracellular antibody cocktail diluted in permeabilisation buffer. Cells were then washed prior to analysis on an Aurora flow cytometer (Cytek Biosciences).

For ILC2 sorting, lineage negative population (CD3ε, CD4, CD8α, CD5, CD19, CD11c, Gr1, F4/80, FcεRIa, NK1.1, CD11b, and TER119) were excluded by Magnetic Cell sorting system (MACS, Miltenyi Biotec) from single-cell suspension. MACS separated cells were blocked with anti-CD16/CD32 for 20 min on ice then stained with CD45, CD127, KLRG1, CD90.2 and lineage

cocktail antibodies for 1 hour on ice. After staining, cells were washed and resuspended in DAPI 5 min prior to sorting and ILC2 cells were sorted on a FACSAria III cell sorter (BD Biosciences).

ILC2 *in vitro* culture and proliferation assay

For each experimental repeat, colons from 15 mice were pooled and sorted as a single sample, and isolated ILC2 cells were split equally between different conditions. ILC2s were cultured for 3 days at 37°C/5% CO2 in U-bottom 96-well plate in complete RPMI medium containing recombinant murine IL-2 (2 ng/ml), IL-7 (5 ng/ml) and either IL-18, IL-22, IL-25, IL-33 or TSLP (100 ng/ml). Cells were re-stained using the extracellular ILC2 marker panel followed by intranuclear Ki67 staining, and cell proliferation was assessed by flow cytometry.

RNA isolation, reverse transcription and quantitative real-time PCR

Total RNA was extracted from IECs or whole tissue using the RNeasy Mini Kit (QIAGEN) and converted to cDNA using iScript cDNA synthesis kit (BIO-RAD) in accordance with the manufacturer's instructions. The RT-qPCR reactions were carried out using the PowerUP SYBR green PCR master mix (Applied Biosystems) and run in duplicates in a 7500 Fast RT-PCR thermocycler (Applied Biosystems). Relative gene expression of *Il18*, *Il25*, *Il33* and *Tslp* was calculated by the comparative cycle threshold (Ct) method $2^{-\Delta\Delta Ct}$, using *Hprt*, *Actb* and *Gapdh* as housekeeping genes. Primer sequences were as follows: *Il18* forward: GACTCTTGCGTCAACTTCAAGG; *Il18* reverse: CAGGCTGTCTTTTGTCAACGA; *Il25* forward: : ACAGGGACTTGAATCGGGTC; *Il25* reverse: TGGTAAAGTGGGACGGAGTTG; *Il33* forward: TCCAACTCCAAGATTTCCCCG; *Il33* reverse: CATGCAGTAGACATGGCAGAA; *Tslp* forward: : ACGGATGGGGCTAACTTACAA and *Tslp* reverse: AGTCCTCGATTTGCTCGAACT.

Cytokine analysis by ELISA

The levels of IL- 4, IL-5, IL-9, IL-13, IL-18, IL-25 and IL-33 were determined using Duoset ELISA kits (R&D Systems). For tissue explant, 1 cm colon fragments were transferred to a 96-well plate containing RPMI buffer supplemented with 10 % fetal bovine serum (FBS), 100 U/ml penicillin, 100 µg/ml streptomycin and incubated in a 37 °C humidified 5 % CO2 incubator for 24 hours. Supernatants from cultured ILC2 or colonic explants were collected, and cytokines were analysed by ELISA (R&D Systems) according to the manufacturer's instructions.

Proteomics data analysis and visualization

The IEC proteomics dataset of 4 and 6 dpi with CRWT was mined from dataset originally deposited in the ProteomeXchange Consortium via the PRIDE partner repository(30) with the data set identifier PXD012031. The normalized and scaled data were used to compute $\log_2$FC compared to uninfected samples. For statistical analysis, $\log_2$(scaled abundance) of proteins was used, using p-value < 0.05 criteria in two-sample t-test in the Perseus software version 2.0.11(31). The data were visualised using the online Phantasus tool version v1.25.4(32).

Statistical analysis

Flow cytometry data were analysed using FLowJo software (Tree Star). Graphs and statistical tests were carried out using GraphPad Prism 10.2.3 software and data were expressed as mean ± SEM. Statistical differences were calculated using the unpaired Mann-Whitney Student's t test for two groups and one-way ANOVA for 3 or more groups. A p value of <0.05 is considered significant, *p<0.05, **p<0.01, ***p<0.001.

Custom images of mice in Fig 4C and graphical abstract were made with Biorender (created with BioRender.com).

Results

C. rodentium infection upregulates mucosal expression of *Il18* and *Il33*

The aim of this study was to determine whether ILC2 respond to enteric bacterial infections, knowing that ILC3s are the predominate ILC subset that is involved in a protective response to such pathogens. To this end, we infected wild type C57Bl/6 female mice with *C. rodentium* by oral gavage. We quantified *C. rodentium* shedding, CCH and inflammation. Enumerating faecal bacterial colony forming units (CFU) revealed that *C. rodentium* was shed at ca. 10^8 CFU/g of stool (Figure 1A). While measuring crypt length in H&E-stained paraffin-embedded colonic sections revealed no significant increase in CCH compared to the controls (Figure 1B and 1C), the colon length of *C. rodentium*-infected mice was significantly shorter than PBS-dosed mice (Figure 1D and 1E). Moreover, faecal myeloperoxidase (MPO), a neutrophil-derived biomarker, and IL-18 secreted from issue explants were significantly higher in infected samples (Figures 1F and 1G). These results show that *C. rodentium* induces signs of colonic inflammation as early as 4 dpi.

While there is a rich literature describing activation of ILC3 early during *C. rodentium* infection, here we evaluated if any of the potential ILC2-activating cytokines are expressed 4 days post *C. rodentium* infection. While qPCR revealed that *Il25* expression did not increase following infection and *TLSP* was not detected, expression of *Il18 and Il33* was elevated in colonic IECs of infected mice (Figure 1H). Consistently, reanalyzing our temporal proteomics from colonic IECs isolated from *C. rodentium*-infected mice at 4 dpi (26) revealed marked elevation of anti-apoptotic protein Bcl2 (Figure 1I), which is regulated by IL-33 (33). In addition, increased abundance of the epidermal growth factor amphiregulin (Areg), regulated by IL-33, IL-25, TSLP, and IL-18 (34, 35) was also observed (Fig. 1I). Moreover, the abundance of the IL-18 regulated proteins

Lysozyme 1 and 2 (Lyz2), iNOS (Nos2) (36), stem cell gene Lgr5 (37), proliferation marker mki67 and MMP9 (38), significantly increased at 4 dpi (26). Conversely, the abundance of proteins repressed by IL-33 (39), such as the pro-apoptotic protein Bax, and caspases (Casp3 and Casp1) decreased (Figure 1I). As we observed clear proteomic IL-18 and IL-33 signatures, we hypothesised that ILC2s are activated during the early stages of *C. rodentium* infection.

Colonic ILC2s proliferate in response to *C. rodentium* infection

We next investigated colonic lamina propria ILC2 cells at 4 dpi; mice dosed with PBS were used as controls. We assessed the numbers and proportions of ILC2, as well as ILC1s and NK cells by flow cytometry, using a combination of CD45, CD90.2, NKp46, KLRG1, CD127, lineage markers, and transcription factors (GATA-3, T-bet, RORγt and EOMES) (Figure S1A). This revealed that the number of ILC1s, NK cells and ILC2s increased upon infection (Figure 2A); while the proportion of ILC1s remained unchanged, that of NK cells and ILC2s increased (Figure 2A). To determine their cytokine profile, colonic lamina propria cells were stimulated *ex vivo* with PMA/ionomycin for 4 h in the presence of a protein transport inhibitor cocktail. As expected, ILC1 and NK cells from infected mice produced higher levels of IFNγ compared to the mock-infected group (Figure 2B-D). We next sorted ILC2s from pooled colons of uninfected and *C. rodentium*-infected female mice (Figure 2E). Upon stimulation with PMA/ionomycin (without protein transport inhibitors), ILC2s from infected mice secreted elevated amounts of IL-5, IL-4 and IL-13 (Figure 2F). When protein transport inhibitor cocktail was present in the stimulation media, IL-5^{+}, IL-4^{+} and IL-13^{+} ILC2 populations were higher in *C. rodentium* infected samples (Figure S1B and S1C). This observation is supported by the increased abundance of proteins regulated by ILC2-secreting cytokines in the 4 dpi proteomics dataset (26), including IL-4 receptor (Il4R), lymphocyte adhesion CD44 (40), Jun, Fos (41), mucin O-glycosylating enzyme (Galnt1 and 11)

(42), Retnlb (RelMβ) involved in host defense (43) and Cldn2 involved in barrier function (44) (Figure 2G).

Colonic ILC2s proliferate in response to IL-18

We investigated if, similarly to lung and skin ILC2s, IL-18 could also stimulate lamina propria ILC2s (45, 46). To this end, we sorted ILC2s from the colons of naive C57Bl/6 female mice and measured their proliferation (ki67) in the presence of IL-18; IL-22 was included as a control. Following *in vitro* stimulation for three days, ILC2s proliferated in response to IL-18, but not IL-22 (Figure 3A-D). As expected, the positive controls IL-25 and IL-33 induced ILC2 proliferation, although the colonic ILC2 cells were unresponsive to TSLP (Figure 3A-D). Analysing supernatants of stimulated ILC2s for cytokine production by ELISA showed that IL-18, IL-25 and IL-33 triggered secretion of IL-5, IL-9, and IL-13, but not IL-4 (Figure 3E).

The administration of IL-18 restored the activation of ILC2s in IL-22 KO mice

IL-22, a key cytokine at the early phase of *C. rodentium* infection, does not activate ILC2, while its downstream cytokine IL-18 does (Figure 3). We therefore investigated whether IL-22 signalling affects expansion and activation of ILCs *in vivo*, particularly ILC2. To this end we infected IL-22 KO male mice with *C. rodentium*, which was shed at ca. 10^8 CFU/g of stool (Figure S2A) and induced shortening of the colon (Figure S2B). No significant increase was seen in CCH (Figure S2C and S2D), whereas MPO levels were significantly higher in IL-22 KO infected mice compared to PBS mock-infected control mice (Figure S2E). Whilst ILC1 and NK cell populations expanded in the *C. rodentium*-infected IL-22 KO mice, ILC2s did not (Figure 4A). We then tested the expression of *Il18* in wild type (WT) and IL-22 KO male mice in uninfected mice at 0 and 4 dpi by qPCR. This showed that IL-22 KO mice had a significant lower expression of *Il18* compared

to WT-infected mice at 4 dpi, while no difference was seen in uninfected mice (Figure 4B). To confirm that IL-18, secreted in response to IL-22, is a trigger of ILC2 proliferation during *C. rodentium* infection, infected IL-22 KO female mice were administered recombinant IL-18 intraperitoneally (Figure 4C). This resulted in expansion of colonic lamina propria ILC2 cells (Figure 4D).

We then performed a reciprocal experiment, where *C. rodentium*-infected wild type female mice were treated with IL-18 binding protein (IL-18BP) intraperitoneally (Figure 4D), at 2 and 3 dpi. Treated mice presented a significantly lower number and frequency of ILC2 cells compared to the vehicle control group (Figure 4E). These findings suggest that IL-18 can stimulate colonic lamina propria ILC2s.

Discussion

While ILC3s are one of the first responders to gut perturbation and infection with extracellular enteric pathogens, ILC2s mainly respond to helminths. In this study we show that lamina propria ILC1s, NK cells and particularly ILC2s are activated during *C. rodentium* infection. ILC2s extracted from the lamina propria of infected mice produced IL-4, IL-5 and IL-13, and are activated primarily by IL-18 and IL33. These results show that in addition to responding to helminth infection, ILC2 are also activated during extracellular bacterial gut infection.

Previous studies have shown the involvement of NK cells in the clearance of *C. rodentium*, in which IFN-γ-producing NK cells expanded within the mesenteric lymph nodes and colonic lamina propria at 2, 7 and 14 dpi, and their depletion led to a higher bacterial load and severe inflammation (47). It has also been reported that ILC1 cells expand in the small intestine of *C. rodentium*-infected mice, suggesting an ILC3/1 plasticity pathway (48).

IL-4, IL-5 and IL-13 are typically linked to barrier function and tissue repair. During helminth infections, IL-13 produced by ILC2s drives goblet cell proliferation, mucus secretion and smooth muscle contractility, contributing to parasite expulsion (14), whereas IL-5 is associated with the recruitment of eosinophils and can also enhance IgA production (13, 49). IL-4, however, plays a role in regulating IgE responses in B cells, the differentiation of alternatively activated M2 macrophages as well as the production of mucus (50). A recent study reported that during *Helicobacter pylori* infection, IL-33 activates stomach ILC2s to secrete IL-5 which resulted in IgA production, controlling bacteria in infected mice (18). The significance of ILC2 activation during *C. rodentium* infection could lie in production of IL-5 and IL-4, which can act synergistically to influence or enhance an antibody response, in addition to IL-13 which drives mucus production,

promoting bacterial clearance (51). Moreover, during parasitic nematode infection, ILC2s have been shown to synthesise and release acetylcholine (ACh) (52), documented to enhance immunity to *C. rodentium* (53). Depleting ACh production in T cells led to a higher bacterial burden and increased levels of IL-1β, IL-6 and TNFα in the gut of *C. rodentium* infected mice (53).

While TSLP has been reported to activate ILC2s (54), IL-25 and IL-33 are the major ILC2 inducers in the gut and lung (17, 55). In this study, TSLP did not activate colonic ILC2s *in vitro*. Importantly, we found that in addition to the alarmins IL-33 and IL-25, IL-18 also induced colonic ILC2s to proliferate and secrete IL-5 and IL-13 *in vitro*. Indeed, skin ILC2 subsets have been shown to be activated dominantly by IL-18 via the IL-18R1 receptor, which is highly expressed in skin ILC2s and can be expressed on lung and bone marrow, but not on small intestine ILC2s (19). Our data suggest that the IL-18R1 receptor is also expressed on ILC2s in the large intestine.

In the context of *C. rodentium* infection, the likely source of IL-18 is IL-22-activated IECs (45). Our data showed that *Il18* and *Il33* expression increased upon *C. rodentium* infection, and elevated levels of secreted IL-18 were detected in explant tissue from infected mice. In addition, the administration of IL-18 to *C. rodentium* infected IL-22 KO mice, restored the expansion of ILC2s in the colonic lamina propria. Accordingly, we propose that IL-18, secreted from IECs in response to IL-22, and IL-33, secreted from epithelial cells due to tissue damage, are the major inducers of ILC2 expansion and activation during *C. rodentium* infection. Further studies are needed to determine the functional role of ILC2s in host responses to *C. rodentium* and how widespread this response is in other bacterial enteric infections.

Acknowledgments

We thank Dr Jessica Rowley and Dr Larissa Zarate Garcia for their technical assistance and support with flow cytometry and cell sorting.

Footnotes

This study was supported by grants from The Wellcome Trust (107057/z/15/z and 224282/Z/21/Z) and the medical research council (MRC) (MR/R02671).

R.B.: Conceptualization, Methodology, Validation, Formal analysis, Investigation, Writing – original draft, Writing – review & editing, Visualization. **V.M.:** Conceptualization, Methodology, Formal analysis, Investigation. **P.B.:** Formal analysis. **Z.K.:** Resources. **J.C.:** Resources**. G.F.**: Conceptualization, Resources, Writing – review & editing, Supervision, Project administration, Funding acquisition.

Abbreviations

Acetylcholine (Ach); Amphiregulin (Areg); Antimicrobial peptides (AMPs); Caspase (Casp); *Citrobacter rodentium* (*C. rodentium*); Colonic crypt hyperplasia (CCH); Colony forming units (CFU); Days post infection (dpi); Granulocyte macrophage colony-stimulating factor (GM-CSF); IL-18 binding protein (IL-18BP); Innate lymphoid cells (ILCs); Interferon gamma (IFNγ); Interleukin (IL); Intestinal epithelial cells (IECs); Knock-out (KO); Lymphoid tissue inducer cells (LTis); Myeloperoxidase (MPO); Natural killer (NK); *Nippostrogylus brasiliensis* (*N. brasiliensis*); Wild-type (WT).

References

1. Artis D, Spits H. The biology of innate lymphoid cells. Nature. 2015;517(7534):293-301.
2. Spits H, Artis D, Colonna M, Diefenbach A, Di Santo JP, Eberl G, et al. Innate lymphoid cells--a proposal for uniform nomenclature. Nat Rev Immunol. 2013;13(2):145-9.
3. Spits H, Di Santo JP. The expanding family of innate lymphoid cells: regulators and effectors of immunity and tissue remodeling. Nat Immunol. 2011;12(1):21-7.
4. Vivier E, Artis D, Colonna M, Diefenbach A, Di Santo JP, Eberl G, et al. Innate Lymphoid Cells: 10 Years On. Cell. 2018;174(5):1054-66.
5. Almeida FF, Belz GT. Innate lymphoid cells: models of plasticity for immune homeostasis and rapid responsiveness in protection. Mucosal Immunol. 2016;9(5):1103-12.
6. Muraoka WT, Korchagina AA, Xia Q, Shein SA, Jing X, Lai Z, et al. Campylobacter infection promotes IFNgamma-dependent intestinal pathology via ILC3 to ILC1 conversion. Mucosal Immunol. 2021;14(3):703-16.
7. Wolf NK, Kissiov DU, Raulet DH. Roles of natural killer cells in immunity to cancer, and applications to immunotherapy. Nature reviews Immunology. 2023;23(2):90-105.
8. Bernink JH, Peters CP, Munneke M, te Velde AA, Meijer SL, Weijer K, et al. Human type 1 innate lymphoid cells accumulate in inflamed mucosal tissues. Nat Immunol. 2013;14(3):221-9.
9. Fuchs A, Vermi W, Lee JS, Lonardi S, Gilfillan S, Newberry RD, et al. Intraepithelial type 1 innate lymphoid cells are a unique subset of IL-12- and IL-15-responsive IFN-gamma-producing cells. Immunity. 2013;38(4):769-81.
10. Gasteiger G, Fan X, Dikiy S, Lee SY, Rudensky AY. Tissue residency of innate lymphoid cells in lymphoid and nonlymphoid organs. Science. 2015;350(6263):981-5.
11. Abt MC, Lewis BB, Caballero S, Xiong H, Carter RA, Susac B, et al. Innate Immune Defenses Mediated by Two ILC Subsets Are Critical for Protection against Acute Clostridium difficile Infection. Cell Host Microbe. 2015;18(1):27-37.
12. Klose CSN, Flach M, Mohle L, Rogell L, Hoyler T, Ebert K, et al. Differentiation of type 1 ILCs from a common progenitor to all helper-like innate lymphoid cell lineages. Cell. 2014;157(2):340-56.
13. Moro K, Yamada T, Tanabe M, Takeuchi T, Ikawa T, Kawamoto H, et al. Innate production of T(H)2 cytokines by adipose tissue-associated c-Kit(+)Sca-1(+) lymphoid cells. Nature. 2010;463(7280):540-4.

14. Price AE, Liang HE, Sullivan BM, Reinhardt RL, Eisley CJ, Erle DJ, et al. Systemically dispersed innate IL-13-expressing cells in type 2 immunity. Proc Natl Acad Sci U S A. 2010;107(25):11489-94.

15. Gerbe F, Sidot E, Smyth DJ, Ohmoto M, Matsumoto I, Dardalhon V, et al. Intestinal epithelial tuft cells initiate type 2 mucosal immunity to helminth parasites. Nature. 2016;529(7585):226-30.

16. Howitt MR, Lavoie S, Michaud M, Blum AM, Tran SV, Weinstock JV, et al. Tuft cells, taste-chemosensory cells, orchestrate parasite type 2 immunity in the gut. Science. 2016;351(6279):1329-33.

17. von Moltke J, Ji M, Liang HE, Locksley RM. Tuft-cell-derived IL-25 regulates an intestinal ILC2-epithelial response circuit. Nature. 2016;529(7585):221-5.

18. Satoh-Takayama N, Kato T, Motomura Y, Kageyama T, Taguchi-Atarashi N, Kinoshita-Daitoku R, et al. Bacteria-Induced Group 2 Innate Lymphoid Cells in the Stomach Provide Immune Protection through Induction of IgA. Immunity. 2020;52(4):635-49 e4.

19. Ricardo-Gonzalez RR, Van Dyken SJ, Schneider C, Lee J, Nussbaum JC, Liang HE, et al. Tissue signals imprint ILC2 identity with anticipatory function. Nat Immunol. 2018;19(10):1093-9.

20. Zeng B, Shi S, Ashworth G, Dong C, Liu J, Xing F. ILC3 function as a double-edged sword in inflammatory bowel diseases. Cell Death Dis. 2019;10(4):315.

21. Collins JW, Keeney KM, Crepin VF, Rathinam VA, Fitzgerald KA, Finlay BB, et al. Citrobacter rodentium: infection, inflammation and the microbiota. Nat Rev Microbiol. 2014;12(9):612-23.

22. Mundy R, MacDonald TT, Dougan G, Frankel G, Wiles S. Citrobacter rodentium of mice and man. Cell Microbiol. 2005;7(12):1697-706.

23. Wang B, Lim JH, Kajikawa T, Li X, Vallance BA, Moutsopoulos NM, et al. Macrophage beta2-Integrins Regulate IL-22 by ILC3s and Protect from Lethal Citrobacter rodentium-Induced Colitis. Cell Rep. 2019;26(6):1614-26 e5.

24. Sonnenberg GF, Fouser LA, Artis D. Border patrol: regulation of immunity, inflammation and tissue homeostasis at barrier surfaces by IL-22. Nat Immunol. 2011;12(5):383-90.

25. Sonnenberg GF, Monticelli LA, Alenghat T, Fung TC, Hutnick NA, Kunisawa J, et al. Innate lymphoid cells promote anatomical containment of lymphoid-resident commensal bacteria. Science. 2012;336(6086):1321-5.

26. Hopkins EGD, Roumeliotis TI, Mullineaux-Sanders C, Choudhary JS, Frankel G. Intestinal Epithelial Cells and the Microbiome Undergo Swift Reprogramming at the Inception of Colonic Citrobacter rodentium Infection. mBio. 2019;10(2).

27. Mullineaux-Sanders C, Kozik Z, Sanchez-Garrido J, Hopkins EGD, Choudhary JS, Frankel G. Citrobacter rodentium Infection Induces Persistent Molecular Changes and Interferon Gamma-Dependent Major Histocompatibility Complex Class II Expression in the Colonic Epithelium. mBio. 2021;13(1):e0323321.

28. Crepin VF, Collins JW, Habibzay M, Frankel G. Citrobacter rodentium mouse model of bacterial infection. Nat Protoc. 2016;11(10):1851-76.

29. Kim E, Tran M, Sun Y, Huh JR. Isolation and analyses of lamina propria lymphocytes from mouse intestines. STAR Protoc. 2022;3(2):101366.

30. Vizcaino JA, Csordas A, Del-Toro N, Dianes JA, Griss J, Lavidas I, et al. 2016 update of the PRIDE database and its related tools. Nucleic Acids Res. 2016;44(22):11033.

31. Tyanova S, Temu T, Sinitcyn P, Carlson A, Hein MY, Geiger T, et al. The Perseus computational platform for comprehensive analysis of (prote)omics data. Nat Methods. 2016;13(9):731-40.

32. Kleverov M, Zenkova D, Kamenev V, Sablina M, Artyomov MN, Sergushichev AA. Phantasus, a web application for visual and interactive gene expression analysis. Elife. 2024;13.

33. Pallett MA, Crepin VF, Serafini N, Habibzay M, Kotik O, Sanchez-Garrido J, et al. Bacterial virulence factor inhibits caspase-4/11 activation in intestinal epithelial cells. Mucosal Immunol. 2017;10(3):602-12.

34. Ebina-Shibuya R, Leonard WJ. Role of thymic stromal lymphopoietin in allergy and beyond. Nat Rev Immunol. 2023;23(1):24-37.

35. Shubin NJ, Clauson M, Niino K, Kasprzak V, Tsuha A, Guga E, et al. Thymic stromal lymphopoietin protects in a model of airway damage and inflammation via regulation of caspase-1 activity and apoptosis inhibition. Mucosal Immunol. 2020;13(4):584-94.

36. Nakamura K, Kassem S, Cleynen A, Chretien ML, Guillerey C, Putz EM, et al. Dysregulated IL-18 Is a Key Driver of Immunosuppression and a Possible Therapeutic Target in the Multiple Myeloma Microenvironment. Cancer Cell. 2018;33(4):634-48 e5.

37. Chiang HY, Lu HH, Sudhakar JN, Chen YW, Shih NS, Weng YT, et al. IL-22 initiates an IL-18-dependent epithelial response circuit to enforce intestinal host defence. Nature communications. 2022;13(1):874.

38. Wang F, Guan M, Wei L, Yan H. IL-18 promotes the secretion of matrix metalloproteinases in human periodontal ligament fibroblasts by activating NF-kappaB signaling. Mol Med Rep. 2019;19(1):703-10.

39. Ruisong M, Xiaorong H, Gangying H, Chunfeng Y, Changjiang Z, Xuefei L, et al. The Protective Role of Interleukin-33 in Myocardial Ischemia and Reperfusion Is Associated with Decreased HMGB1 Expression and Up-Regulation of the P38 MAPK Signaling Pathway. PLoS One. 2015;10(11):e0143064.

40. Macdonald DC, Leir SH, Brooks C, Sanders E, Lackie P, Rosenberg W. CD44 isoform expression on colonic epithelium mediates lamina propria lymphocyte adhesion and is controlled by Th1 and Th2 cytokines. Eur J Gastroenterol Hepatol. 2003;15(10):1101-10.

41. Kouro T, Takatsu K. IL-5- and eosinophil-mediated inflammation: from discovery to therapy. Int Immunol. 2009;21(12):1303-9.

42. Kanoh A, Takeuchi H, Kato K, Waki M, Usami K, Irimura T. Interleukin-4 induces specific pp-GalNAc-T expression and alterations in mucin O-glycosylation in colonic epithelial cells. Biochim Biophys Acta. 2008;1780(3):577-84.

43. Herbert DR, Yang JQ, Hogan SP, Groschwitz K, Khodoun M, Munitz A, et al. Intestinal epithelial cell secretion of RELM-beta protects against gastrointestinal worm infection. J Exp Med. 2009;206(13):2947-57.

44. Vornewald PM, Forman R, Yao R, Parmar N, Lindholm HT, Lee LSK, et al. Mmp17-deficient mice exhibit heightened goblet cell effector expression in the colon and increased resistance to chronic Trichuris muris infection. Front Immunol. 2023;14:1243528.

45. Munoz M, Eidenschenk C, Ota N, Wong K, Lohmann U, Kuhl AA, et al. Interleukin-22 induces interleukin-18 expression from epithelial cells during intestinal infection. Immunity. 2015;42(2):321-31.

46. Valle-Noguera A, Sancho-Temino L, Castillo-Gonzalez R, Villa-Gomez C, Gomez-Sanchez MJ, Ochoa-Ramos A, et al. IL-18-induced HIF-1alpha in ILC3s ameliorates the inflammation of C. rodentium-induced colitis. Cell Rep. 2023;42(12):113508.

47. Hall LJ, Murphy CT, Hurley G, Quinlan A, Shanahan F, Nally K, et al. Natural killer cells protect against mucosal and systemic infection with the enteric pathogen Citrobacter rodentium. Infection and immunity. 2013;81(2):460-9.

48. Sepahi A, Liu Q, Friesen L, Kim CH. Dietary fiber metabolites regulate innate lymphoid cell responses. Mucosal Immunol. 2021;14(2):317-30.

49. Yasuda K, Muto T, Kawagoe T, Matsumoto M, Sasaki Y, Matsushita K, et al. Contribution of IL-33-activated type II innate lymphoid cells to pulmonary eosinophilia in intestinal nematode-infected mice. Proc Natl Acad Sci U S A. 2012;109(9):3451-6.

50. Varela F, Symowski C, Pollock J, Wirtz S, Voehringer D. IL-4/IL-13-producing ILC2s are required for timely control of intestinal helminth infection in mice. Eur J Immunol. 2022;52(12):1925-33.

51. Gustafsson JK, Navabi N, Rodriguez-Pineiro AM, Alomran AH, Premaratne P, Fernandez HR, et al. Dynamic changes in mucus thickness and ion secretion during Citrobacter rodentium infection and clearance. PloS one. 2013;8(12):e84430.

52. Roberts LB, Schnoeller C, Berkachy R, Darby M, Pillaye J, Oudhoff MJ, et al. Acetylcholine production by group 2 innate lymphoid cells promotes mucosal immunity to helminths. Sci Immunol. 2021;6(57).

53. Ramirez VT, Godinez DR, Brust-Mascher I, Nonnecke EB, Castillo PA, Gardner MB, et al. T-cell derived acetylcholine aids host defenses during enteric bacterial infection with Citrobacter rodentium. PLoS pathogens. 2019;15(4):e1007719.

54. Kabata H, Flamar AL, Mahlakoiv T, Moriyama S, Rodewald HR, Ziegler SF, et al. Targeted deletion of the TSLP receptor reveals cellular mechanisms that promote type 2 airway inflammation. Mucosal Immunol. 2020;13(4):626-36.

55. Kim HY, Chang YJ, Subramanian S, Lee HH, Albacker LA, Matangkasombut P, et al. Innate lymphoid cells responding to IL-33 mediate airway hyperreactivity independently of adaptive immunity. J Allergy Clin Immunol. 2012;129(1):216-27 e1-6.

Disclosures

The authors have no financial conflicts of interest.

Figure Legends

Figure 1. *C. rodentium* infection upregulates mucosal expression of *Il18* and *Il33*. A. Colonisation of *C. rodentium* (CR) determined in faecal samples at 4 dpi. Mock infected (PBS) were used as controls. **B.** Crypt lengths measured from H&E-stained colon sections. **C.** Representative H&E sections from the distal colons of uninfected (PBS) and infected mice at 4 dpi (scale bar 100 μm). **D.** Representative and **E.** quantitative figure of colon length. **F.** Faecal MPO levels measured by ELISA. **F.** IL-18 levels detected by ELISA on explant colonic tissue incubated *in vitro* for 24 h. **G.** RT-qPCR analysis of *Il18, Il25* and *Il33* transcript expression in enriched IECs from colons of CR-infected and PBS-dosed mice at 4 dpi. Each data point represents one mouse. **I.** Heatmap of selected proteins in IECs from C57BL/6 mice infected with *C. rodentium* at 4 dpi. Log_2FC (compared to UI samples) of proteins involved in IL-18, IL-33, IL-25, and TSLP response. dpi: days post infection, FC: fold change. Data are represented as mean ± SEM.

Figure 2. ILC populations on day 4 post *C. rodentium* infection. A. Numbers of ILC1, ILC2 and NK cells increased upon infection, as well as the frequency of NK cells and ILC2s. **B.** Representative flow cytometry plots of cytokine expression from fluorescent-minus-one (FMO), unstimulated and stimulated samples. **C.** $IFN\gamma^+$ ILC1s and **D.** $IFN\gamma^+$ NK cells of stimulated lamina propria cells increased in *C. rodentium* infected mice. **E.** Total ILC2 numbers sorted from pooled colons of uninfected and infected mice. **F.** IL-4, IL-5 and IL-13 levels in the supernatant from the same sorted cells measured by ELISA. **G.** Heatmap of selected proteins in IECs from C57BL/6

mice infected with *C. rodentium* at 4 dpi or that of mock-infected controls. Log_2FC (compared to uninfected samples) of proteins involved in IL-4, IL-5, and IL-13 response. dpi: days post infection, FC: fold change. Data shown are mean ± SEM from three independent experiments. See also Figure S1.

Figure 3. Colonic lamina propria ILC2s proliferate in response to IL-18. A. Representative flow cytometry plots and **B.** Summary data for Ki67 expression (represented as percentage of ILC2) by FACS sorted colonic lamina propria ILC2s. Cells were cultured for 3 days *in vitro* with recombinant IL-2 and IL-7 (control) in addition to IL-22, IL-18, Il-25, IL-33 or TSLP. **C.** Histogram and **D.** MFI summary data showing positive and negative peaks of proliferative ILC2s in response to different cytokines. **E.** IL-5, IL-9 and IL-13 levels in the supernatant from cultured ILC2s measured by ELISA. Cells pooled from n = 10 mice per experiment. Data shown are mean ± SEM from four independent experiments.

Figure 4. IL-18 restored the stimulation of ILC2s in IL-22 KO mice. A. Frequency and absolute number of ILC1, ILC2 and NK cells in the colon of PBS and CR infected IL-22KO mice. **B.** Relative expression of *Il18* mRNA normalised to *Gapdh* in the distal colon of WT and IL-22 KO mice over the course of *C. rodentium* infection. **C.** Experimental plan**. D.** ILC2 expansion is restored in the colon of CR infected IL-22 KO mice after IL-18 administration. **E.** Frequency and absolute number of ILC2s is reduced in the colon of CR infected C57BL/6J mice when treated with IL-18BP. Data shown are mean ± SEM from three independent experiments. See also Figure S2.

Fig. 1

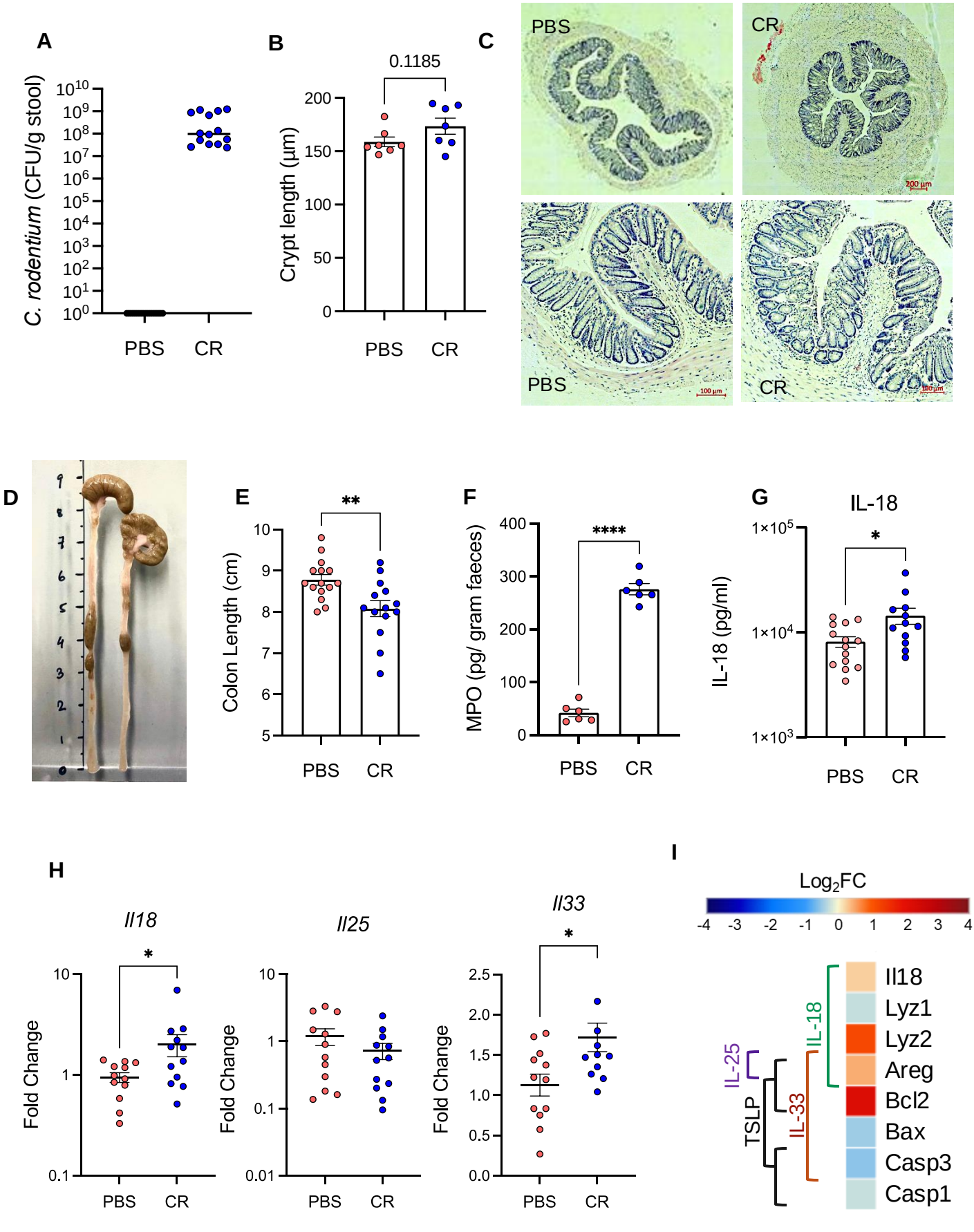
A
C. rodentium (CFU/g stool)
PBS
CR
B
0.1185
Crypt length (µm)
PBS
CR
C
PBS
CR
PBS
CR
D
E
**
Colon Length (cm)
PBS
CR
F
****
MPO (pg/ gram faeces)
PBS
CR
G
IL-18
*
IL-18 (pg/ml)
PBS
CR
H
Il18
*
Fold Change
PBS
CR
Il25
Fold Change
PBS
CR
Il33
*
Fold Change
PBS
CR
I
Log2FC
-4 -3 -2 -1 0 1 2 3 4
IL-25
TSLP
IL-33
IL-18
Il18
Lyz1
Lyz2
Areg
Bcl2
Bax
Casp3
Casp1

Fig. 2

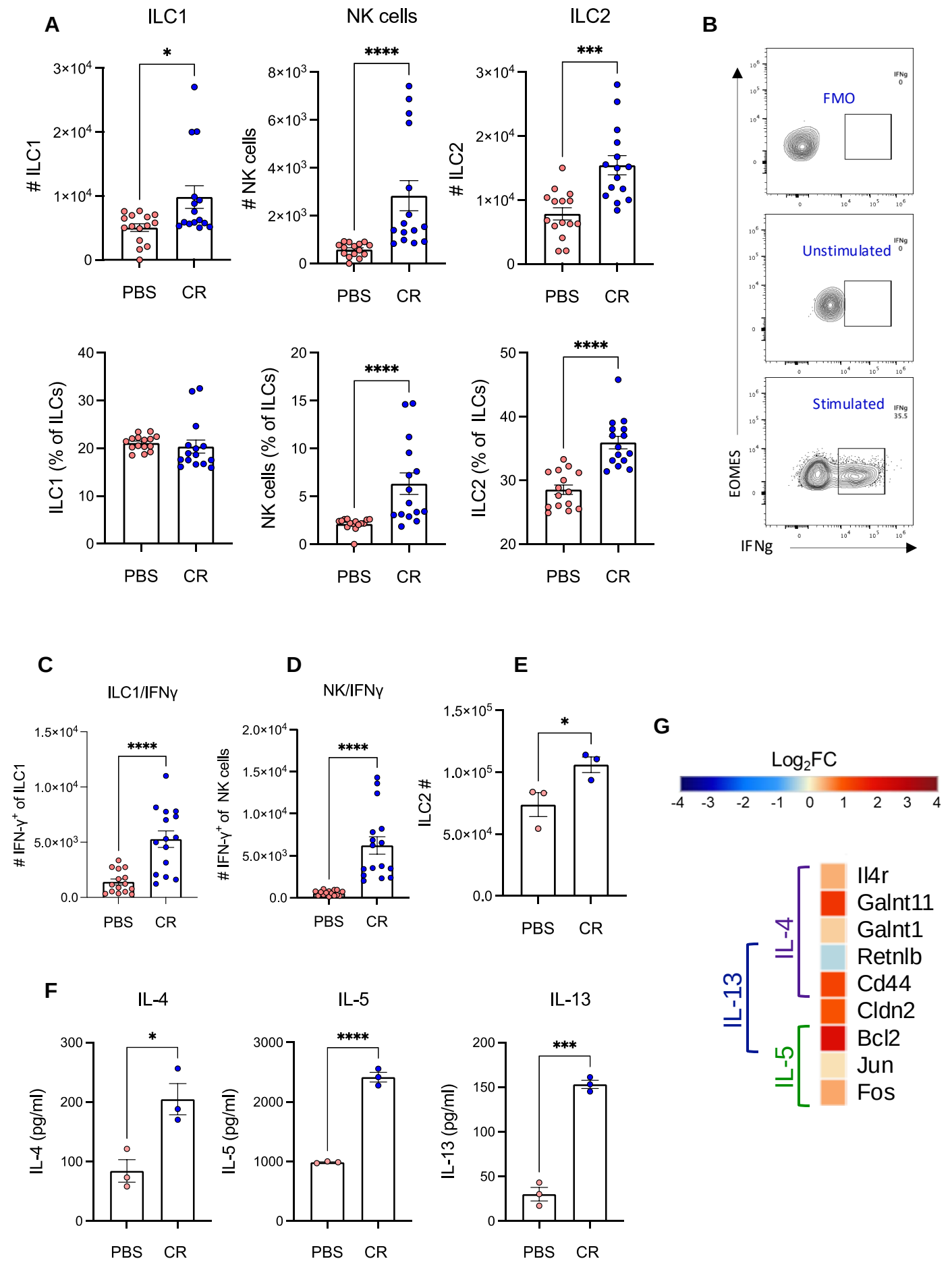
A
ILC1
NK cells
ILC2
ILC1
NK cells
ILC2
ILC1 (% of ILCs)
NK cells (% of ILCs)
ILC2 (% of ILCs)
PBS
CR
B
FMO
Unstimulated
Stimulated
EOMES
IFNg
C
ILC1/IFNγ
IFN-γ+ of ILC1
D
NK/IFNγ
IFN-γ+ of NK cells
E
ILC2 #
G
Log2FC
-4 -3 -2 -1 0 1 2 3 4
Il4r
Galnt11
Galnt1
Retnlb
Cd44
Cldn2
Bcl2
Jun
Fos
IL-4
IL-13
IL-5
F
IL-4
IL-5
IL-13
IL-4 (pg/ml)
IL-5 (pg/ml)
IL-13 (pg/ml)

Fig. 3

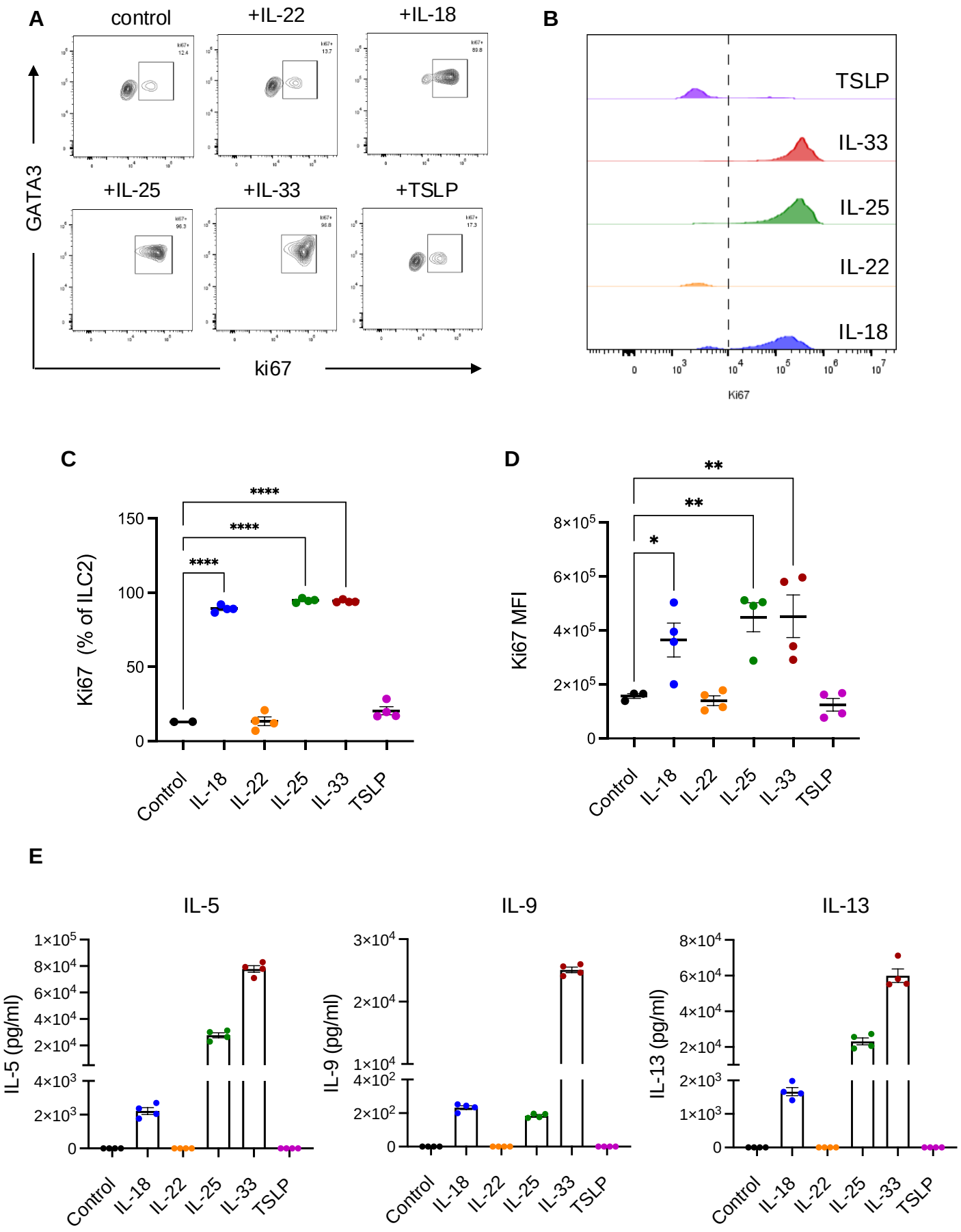
A
control
+IL-22
+IL-18
+IL-25
+IL-33
+TSLP
GATA3
ki67
B
TSLP
IL-33
IL-25
IL-22
IL-18
Ki67
C
Ki67 (% of ILC2)
Control
IL-18
IL-22
IL-25
IL-33
TSLP
D
Ki67 MFI
E
IL-5
IL-9
IL-13
IL-5 (pg/ml)
IL-9 (pg/ml)
IL-13 (pg/ml)

Fig. 4

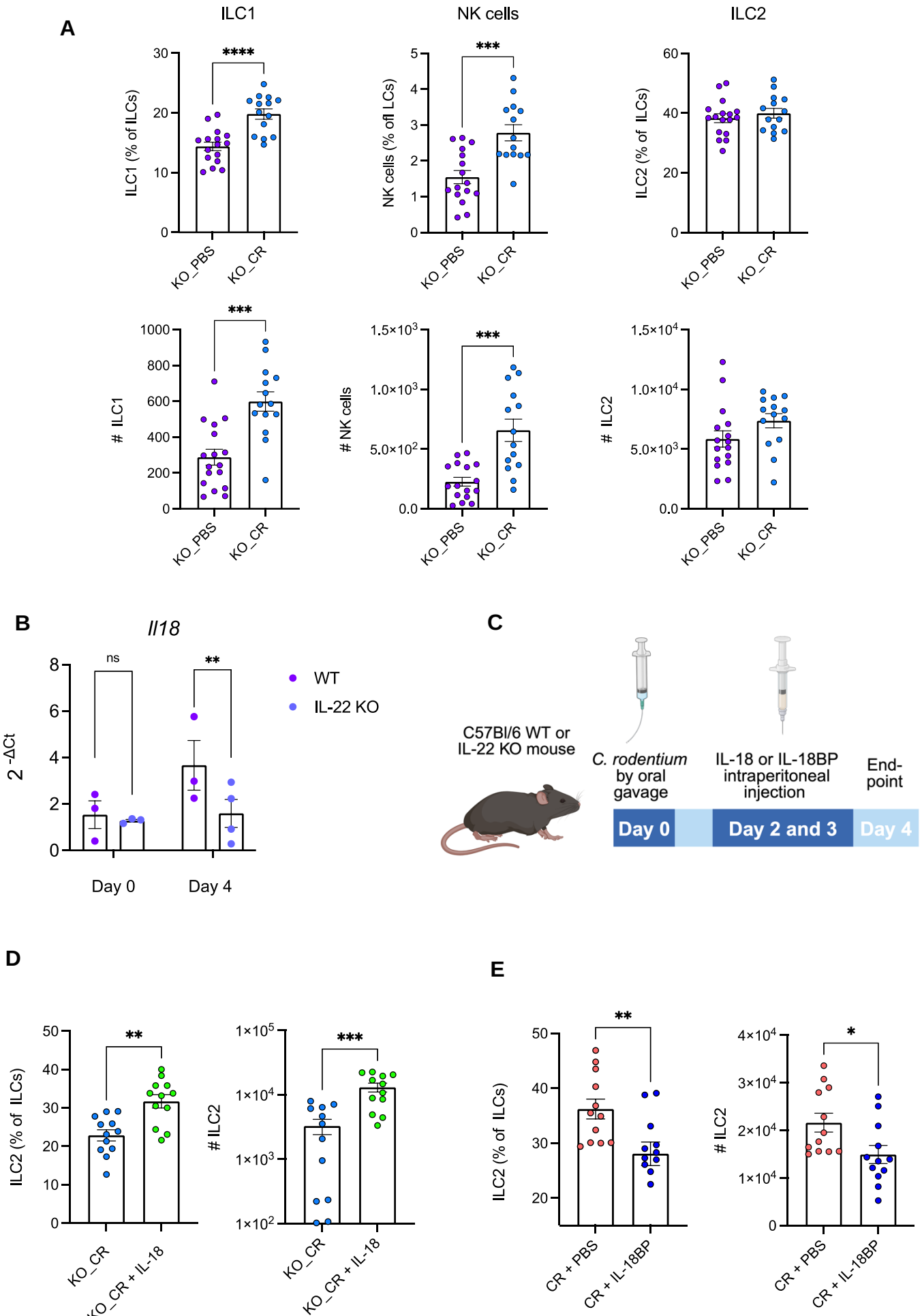
A
ILC1
NK cells
ILC2
ILC1 (% of ILCs)
NK cells (% ofl LCs)
ILC2 (% of ILCs)
ILC1
NK cells
ILC2
KO_PBS
KO_CR
B
Il18
2 -ΔCt
ns
WT
IL-22 KO
Day 0
Day 4
C
C57Bl/6 WT or IL-22 KO mouse
C. rodentium by oral gavage
IL-18 or IL-18BP intraperitoneal injection
End-point
Day 0
Day 2 and 3
Day 4
D
ILC2 (% of ILCs)
ILC2
KO_CR
KO_CR + IL-18
E
ILC2 (% of ILCs)
ILC2
CR + PBS
CR + IL-18BP